PHYSICAL REVIEW B **95**, 161111(R) (2017)

Non-Abelian $\nu = \frac{1}{2}$ quantum Hall state in Γ_8 valence band hole liquid

George Simion* and Yuli Lyanda-Geller†

Department of Physics and Astronomy and Purdue Quantum Center, Purdue University, West Lafayette, Indiana 47907, USA

(Received 31 March 2016; revised manuscript received 6 February 2017; published 21 April 2017)

In the search for states with non-Abelian statistics, we explore the fractional quantum Hall effect in a system of two-dimensional (2D) charge carrier holes. We propose a method of mapping states of holes confined to a finite width quantum well in a perpendicular magnetic field to states in a spherical shell geometry. We take into account strong coupling between the spin and motion of charge parallel and perpendicular to the 2D layer. This method gives the single-particle hole states used in the exact diagonalization of systems with a small number of holes in the presence of Coulomb interactions, density matrix renormalization group, and topological entanglement entropy calculations. The hole quantum Hall state at half filling of the ground state in a magnetic field near the crossing of single-hole states is likely the Moore-Read Pfaffian state.

DOI: 10.1103/PhysRevB.95.161111

Non-Abelian statistics paves the way to fault-tolerant quantum computing [1–3]. States with non-Abelian excitations can arise in two-dimensional (2D) quantum liquids in magnetic fields. The fractional quantum Hall (FQH) electron state at a filling factor $\nu = \frac{5}{2}$, most studied theoretically and experimentally [4–9], is possibly such a state. Non-Abelian excitations were discussed for $\nu = \frac{12}{5}$, $\nu = \frac{8}{3}$, and $\nu = \frac{1}{4}$ FQH states [10–14], and the bilayer $\nu = \frac{1}{2}$ 2D electron state [15–18].

Here, we show that the fractional quantum Hall effect (FQHE) of 2D holes is a different non-Abelian system. Luttinger valence band holes differ fundamentally from electrons. They exhibit non-Abelian phases in transport even for single-hole states [19]. In a magnetic field, the single-hole states are four-component spinors with each component given by a distinct Landau level (LL) wave function u_n, $n \geqslant 0$. The relative weights of u_n in spinors vary with magnetic field [20] or with strain, driving transitions between, e.g., the Laughlin $\nu = \frac{1}{3}$ state and gapless states [21]. The non-Laughlin FQH electron correlations [22] arise in LL1 due to u_1. For holes, the ground state is often defined by $u_{n\neq 0}$, including u_1. Thus, the non-Abelian FQH hole states can arise when only the ground level in a single quantum well is filled.

Single-hole spectra show multiple level crossings, e.g., in the ground state. Near the crossings, the interaction pseudopotentials can be easily tuned. This can lead to Moore-Read [4] or anti-Pfaffian states [23], such as for electrons at $\nu = \frac{5}{2}$ [24]. The crossing of electron levels dominated by u_0 and u_1 is important at $\nu = \frac{2}{5}$ [2], but such electron cases are rare. Hole level crossings are numerous, and the phase diagram is richer compared to electrons.

We propose a theoretical framework for FQHE in hole systems. Unusual hole spectra in a magnetic field stem from a strong spin-orbit coupling between the in-plane and z-direction motion in a quantum well. For electrons, including multicomponent systems [25–28], these degrees of freedom are independent. It is then possible to use the Haldane technique [29] on a sphere in a monopole magnetic field. Hole four-spinors and the inseparability of the in-plane and z-direction motion make the treatment of Coulomb interactions challenging. The Haldane sphere cannot be used for holes. We propose a method for holes in a spherical shell geometry (Fig. 1) and study the many-body wave functions and topological entanglement entropy. We investigate the $\nu = \frac{1}{2}$ hole system and show that it is not in the Halperin 331 FQH state [30] but in a Moore-Read (MR) state.

Holes in the spherical shell geometry. The Luttinger Hamiltonian [31] in magnetic field $\mathbf{B}$ is

$$\hat{H}_0 = \left(\gamma_1 + \frac{5}{2}\gamma\right)\frac{\hat{\mathbf{k}}^2}{2} I - \gamma(\hat{\mathbf{k}}\cdot\mathbf{s})^2 - \left(\frac{\gamma}{2} + \kappa\right)s_z, \quad (1)$$

where energies are in units of $\hbar\omega_c^0 = \hbar eB/m_0 c$, coordinates $\mathbf{r}$ are in units of magnetic length ($\ell = \sqrt{\hbar c/eB}$), wave vectors $\mathbf{k} = -i\nabla_{\mathbf{r}} + e\ell\mathbf{A}/(\hbar c)$, $\mathbf{A}$ is the vector potential, $\mathbf{s}$ is the spin-$\frac{3}{2}$ operator, and γ_1, γ, and κ are isotropic Luttinger parameters. $\hat{H}_0$ commutes with the z projection of the total angular momentum $j_z = l_z + s_z$, and l is the angular momentum. In the symmetric gauge, the hole wave functions in a quantum well of width L are

$$\Psi_{n,m}^{\{\alpha\}} = \begin{pmatrix} \zeta_0^{\{\alpha\}}(z)u_{n,m} \\ \zeta_1^{\{\alpha\}}(z)u_{n-1,m+1} \\ \zeta_2^{\{\alpha\}}(z)u_{n-2,m+2} \\ \zeta_3^{\{\alpha\}}(z)u_{n-3,m+3} \end{pmatrix}, \quad (2)$$

where $u_{n,m}$ are symmetric eigenfunctions [32], and $\zeta(z)$ stems from $\Psi(\pm L/2) = 0$. Index α describes the size quantization and odd/even inversion parity about $z = 0$. Energies and wave functions scale with $w = L/(2\lambda)$ [20]. For $n < 3$, $\Psi_{n,m}^{\{\alpha\}}$ vanish for $n - l < 0$, $l = 1,2,3$. For holes, the finite well width is intrinsically important, because of the strong coupling of spin, 2D, and z-direction motions. This coupling distinguishes our case from exact diagonalization with finite width on the sphere [33].

Constructing states with translationally invariant wave functions, we confine holes to a spherical shell with radius $R_0 - \delta_R \leqslant r \leqslant R_0 + \delta_R$, as shown in Fig. 1(a). A magnetic field $B = 2Qhc/(4\pi er^2)$ is related to an integer monopole of strength $2Q$, and the magnetic flux through spherical surfaces around it is $\phi = 2Qhc/e$. Because $\mathbf{j} = \mathbf{l} + \mathbf{s}$ is a good quantum number for single-hole states, the eigenfunctions of (1) for

*simion@purdue.edu
†yuli@purdue.edu

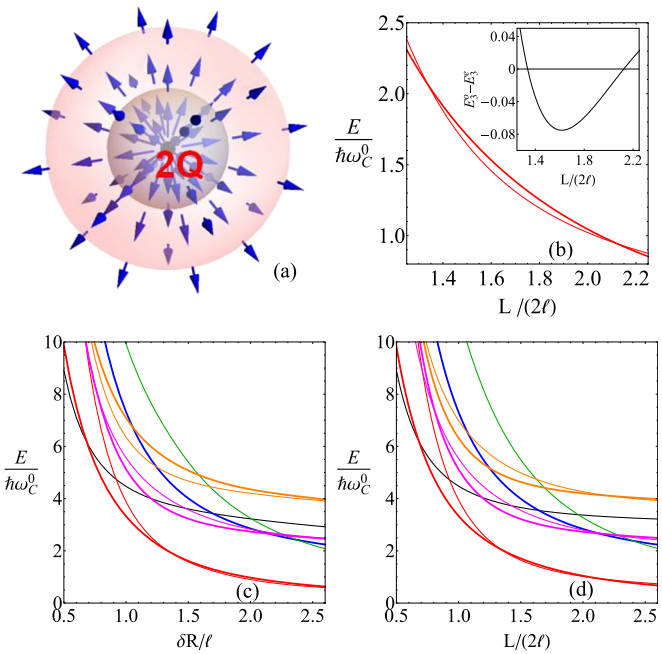

FIG. 1. (a) Spherical shell geometry; (b) ground level crossings in a spherical shell (red solid lines) and planar geometry (black dotted lines); (c), (d) lowest nine states ($n \leqslant 5$) in a (c) spherical shell and (d) planar geometry. The highest index Landau wave function of the shown hole states: black lines, u_0; blue, u_1; green, u_2; red, u_3; magenta, u_4; orange, u_5. Thick lines, even states; thin lines, odd states. The thin red line state has a significant u_1 component.

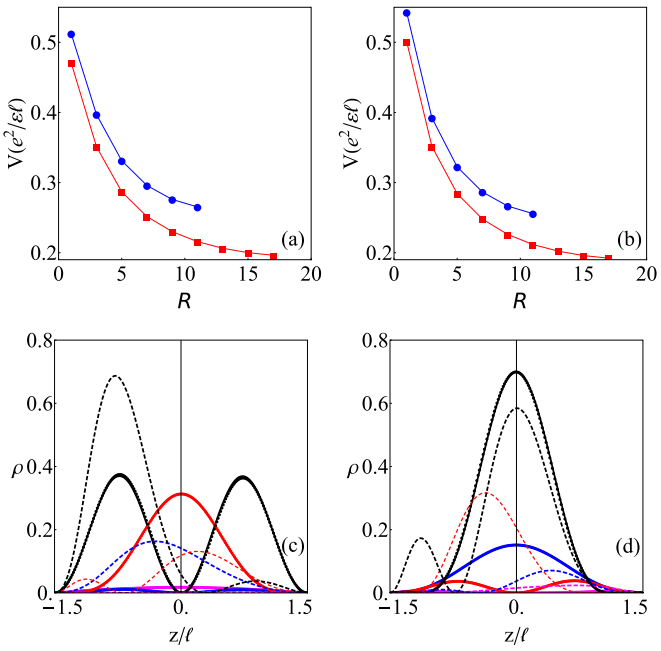

FIG. 2. (a), (b) Pseudopotentials for $w = 1.6$ for $2Q = 10$ (blue dots) and $2Q = 15$ (red squares) for the (a) odd $n = 3$ state and (b) even $n = 3$ state. (c), (d) The charge density ρ. The vertical axis is for the (c) odd $n = 3$ state and for the (d) even $n = 3$ state. Black line: $-\frac{3}{2}$ spin component, which contains $u_0(r)$; red line: $-\frac{1}{2}$ spin component, which contains $u_1(r)$; magenta: $\frac{1}{2}$ spin component, which contains $u_2(r)$; blue: spin $\frac{3}{2}$, which contains $u_3(r)$. The odd $n = 3$ state, which is the ground state between crossings in Fig. 1(b), has the biggest u_1 admixture, and its pseudopotential resembles that of LL1 electrons. In (c) and (d) the solid lines are for the planar case, dashed lines are for $Q = 15$, and dotted lines with $Q = 10^8$ merge with the solid lines.

spherical shell are

$$\psi_{\alpha jm}(r,\theta,\phi) = \sum_{l=j-\frac{3}{2}}^{l=j+\frac{3}{2}} R^l_{\alpha j}(r) \times \begin{pmatrix} \langle j,m|l,m-\frac{3}{2};\frac{3}{2},+\frac{3}{2}\rangle Y_{Q,l,m-\frac{3}{2}}(\theta,\phi) \\ \langle j,m|l,m-\frac{1}{2};\frac{3}{2},+\frac{1}{2}\rangle Y_{Q,l,m-\frac{1}{2}}(\theta,\phi) \\ \langle j,m|l,m+\frac{1}{2};\frac{3}{2},-\frac{1}{2}\rangle Y_{Q,l,m+\frac{1}{2}}(\theta,\phi) \\ \langle j,m|l,m+\frac{3}{2};\frac{3}{2},-\frac{3}{2}\rangle Y_{Q,l,m+\frac{3}{2}}(\theta,\phi) \end{pmatrix}, \tag{3}$$

where $\langle j,m_j|l,m-l;\frac{3}{2},m_s\rangle$ are the Clebsch-Gordan coefficients of $\mathbf{j} = \mathbf{l} + \mathbf{s}$, $Y_{Q,l,m}$ are the monopole harmonics [34], and α labels subbands. Radial functions $R^l_{\alpha j}(r)$ are defined by $\psi_{\alpha jm}(R_0 \pm \delta_R) = 0$. The wave function (3) contains four spinors, each with four components. $Y_{Q,l,m}$ are defined if $l \geqslant Q$ [34], so $2j \geqslant 2Q - 3$. Figures 1(c) and 1(d) show hole spectra in spherical and layer geometries. Figures 2(c) and 2(d) show radial charge distributions for the lowest states. The 2D layer and spherical shell spectra are nearly identical, and crossings of the corresponding states occur almost at the same w. In much the same way as for the Haldane sphere, there are finite size effects, but the shell spectra and the charge density converge to the layer limit for large Q. Thus, we mapped layer holes over a spherical shell. Each spherical state with total angular momentum j corresponds to a layer state with $n = j - Q + \frac{3}{2}$. Each spinor of the spherical wave functions with an angular momentum l corresponds to a spin component in the layer with $s_z = j - l$, and $R^l_{\alpha j}(r)$ are spherical equivalents of $\zeta(z)$. Hole states mix various $u_n(r)$. The weights of u_n in (3) and the average spin of states depend on w, and can be sizably varied by changing the magnetic field.

Coulomb interactions. The Coulomb interactions $H_i = \sum_{ij} \frac{e^2}{\epsilon r_{ij}}$ are treated nonperturbatively. The many-body basis is given by wave functions obtained when N holes are placed in single-particle states (3) in a spherical shell geometry. The integral of motion in a many-body hole system is the total angular momentum $\mathbf{J} = \sum_i \mathbf{j}_i$ and its z projection. We apply the Wigner-Eckart theorem [35]

$$\langle J',M',\beta'|H_i|J,M,\beta\rangle = \delta_{JJ'}\delta_{MM'}V_{\beta\beta'}(\mathcal{J}), \tag{4}$$

and reduce the Hilbert space by using the independence of the interaction matrix elements on J_z. Here, index β labels the multiplets with the same total J and M, and $V_{\beta\beta'}(J) = \langle J',\beta'|H_i|J,\beta\rangle$ are the pseudopotentials [29]. We first compute the main contribution to the two-body pseudopotentials of two holes, each with an angular momentum j, without including virtual transitions to other states, $V^0_{00}(\mathcal{J} = \mathbf{j} + \mathbf{j}) \equiv V_0(\mathcal{R})$, where $\mathcal{R} = j_1 + j_2 - J$ is the relative angular momentum. For the two-body interactions, there is one multiplet for each allowed $\mathcal{J}$. The two-hole pseudopotentials $V_0(\mathcal{R})$ are shown in Figs. 2(a) and 2(b) for holes whose wave functions are the

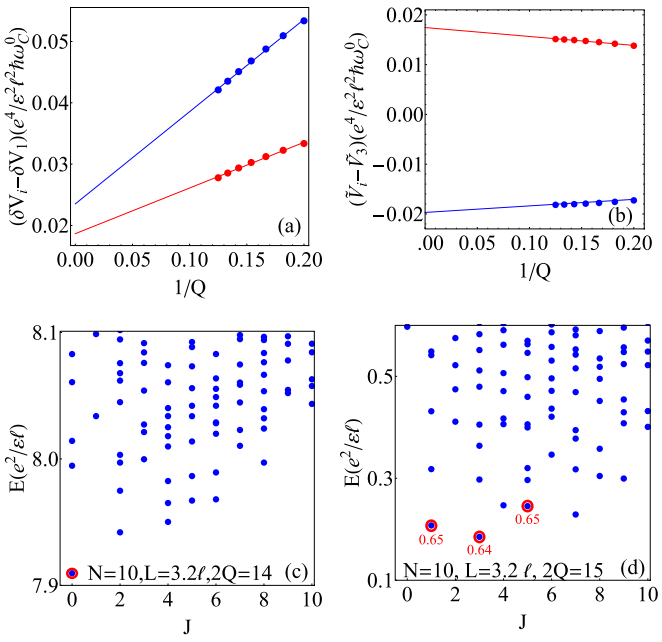

FIG. 3. (a) LL mixing corrections to the two-hole pseudopotentials. Red: $\delta V(\mathcal{R}=3) - \delta V(\mathcal{R}=1)$; blue: $\delta V(\mathcal{R}=5) - \delta V(\mathcal{R}=1)$, $w = 1.6$. (b) Three-hole irreducible pseudopotentials. Red: $\tilde{V}(\mathcal{R}_3=5) - \tilde{V}(\mathcal{R}_3=3)$; blue: $\tilde{V}(\mathcal{R}_3=6) - \tilde{V}(\mathcal{R}_3=3)$, $w = 1.6$. (c) Spectra for ten holes at $\nu = \frac{1}{2}$. The $J = 0$ ground state (red circle) separated by a gap indicates an incompressible state. (d) Pair quasihole excitations of the $\nu = \frac{1}{2}$ state for $N = 10$. The values of overlap between low lying excitations (red circles) and the Moore-Read excitations are shown.

spherical shell counterparts of the odd $n = 3$ and the even $n = 3$ layer states, correspondingly.

Landau level mixing. The hole LL mixing parameter $e^2/(\epsilon\ell\hbar\omega_C)$ is large, so we include virtual transitions to other states [36,37]. In the two-hole states with $\mathcal{J}$, both holes are in the same single-hole state. We diagonalize the system in this basis with the lowest energy acting as an effective interaction. We include virtual transitions into 17 excited states that span the energy range $4\hbar\omega_C$ [38] due to a nonregular separation between hole states. The results are corrections δV to the two-hole pseudopotentials $V_0(\mathcal{R})$. Differences between δV at different $\mathcal{R}$ in units of $e^4/(\ell\epsilon)^2/(\hbar\omega_C^0)$ are shown in Fig. 3(a).

The three-body pseudopotentials $V_{00}(\mathcal{J})$, $\mathcal{J} = \mathbf{j} + \mathbf{j} + \mathbf{j}$, are due to LL mixing. At $\mathcal{R}_3 = 3j - J < 9$ there is one multiplet at each value of $\mathcal{J}$. The effective three-body pseudopotential is found using a basis set made of the three-hole states, which comprised single-hole states with energy $<4\hbar\omega_C$. We extract its irreducible part $\tilde{V}(\mathcal{R}_3)$ as for electrons [39], by subtracting the ground-state energy of a three-hole system, whose interactions are given by the two-body pseudopotentials above. Differences between $\tilde{V}$ at different $\mathcal{R}_3$ in units of $e^4/(\ell\epsilon)^2/(\hbar\omega_C^0)$ are shown in Fig. 3(b). See the Supplemental Material [40].

Hole FQHE at $\nu = \frac{1}{2}$. Simulating N holes at $\nu = \frac{1}{2}$ on a spherical shell at a total angular momentum j given by $2j = 2N - 3$, and magnetic monopole $2Q = 2j - 3$, we obtain a ground state $J = 0$ separated by the gap from the excited states for $N = 6$, 8, 10, 12, 14, and 16. Simulating $N = 6$ and $N = 12$ systems can describe $\nu = \frac{2}{3}$ and $\nu = \frac{3}{5}$, respectively, besides $\nu = \frac{1}{2}$, and we use only $N = 8$, 10, 14, and 16 results. The gaps indicate an incompressible FQH state, as for electrons [41–43]. Figure 3(c) shows the $N = 10$ spectrum. The incompressible state for holes persists in the entire range $1.4 < w < 2.2$ including crossings of the ground odd and even $n = 3$ levels. The maximal gap occurs at $w = 1.6$, as in experiments [44]. For understanding correlations in an incompressible state, we calculate the many-body wave functions and density matrix, the topological entanglement entropy, and the overlap with the wave functions of the model states.

We examine whether the FQH state in experiments [44] is the 331 state. The Halperin 331 state arises for two species of interacting electrons. The wave function of the model 331 state was found in Ref. [45], and for bilayer electrons in Ref. [17]. For the 331 state of holes at $\nu = \frac{1}{2}$, the many-body Hilbert space is made using the $n = 3$ odd and even states. Its size is very large ($\approx 10^6$ for ten particles). The calculated wave-function overlap of the $J = 0$ ground state with the 331 state [45] is only 0.165–0.17 for all fields giving an incompressible state. It was suggested for bilayers [46] that no interlayer tunneling favors the 331 state. For holes, crossings correspond to no single-hole tunneling. However, mixing induced by hole-hole interactions due to the nonconservation of the "pseudospin" comprising $n = 3$ odd and even states takes the role of tunneling and precludes the 331 state.

The MR state is favored by a sizable weight of u_1 and by an average spin ~ -1 of both $n = 3$ states. We test the MR state of $\nu = \frac{1}{2}$ holes using (i) a Hilbert space built using the ground state away from degeneracies, and (ii) a Hilbert space made of both $n = 3$ states. In case (i) we include LL mixing accounting for all higher states, and in case (ii), the closest state to the ground state is included exactly. Using the obtained wave functions, we find overlaps of the model MR ground state [47] with the ground-state wave functions in eight to 16 hole systems ranging from 0.8 to 0.6. We also examine the excitations [Fig. 3(d)]. Removing one flux quantum in the ground state gives two quasielectrons in a hole system, and adding flux quantum creates two quasihole excitations. The MR quasiholes obey non-Abelian statistics [4]. We find the overlap of the wave functions of quasiholes in the $\nu = \frac{1}{2}$, $N = 10$ hole system with the wave functions of MR quasiholes ~ 0.65.

Topological entanglement entropy for $\nu = \frac{1}{2}$ *holes.* The universal aspects of the FQHE are efficiently revealed by investigating the entanglement properties of ground states [48–52]. Entanglement entropy gives a measure of the correlations in FQHE. The system is partitioned in blocks A and B, and the reduced density matrix ρ_A is computed by tracing over B degrees of freedom. Bipartite topological entropy is $S_A = -\mathrm{Tr}\,\rho_A \ln \rho_A$. 2D systems exhibit topologically ordered states with correlations not contained in the usual correlation functions. It was shown that for these states, $S_A = \alpha L - \Gamma + O(L^{-1})$, where L is the length of the boundary between A and B, and α is a nonuniversal constant. The Γ term is the topological entanglement entropy (TEE), which is the logarithm of the inverse quantum dimension [48–52]. This method was applied successfully to probe the Laughlin correlations at $\nu = 1/m$ and MR correlations at $\nu = \frac{5}{2}$ [53].

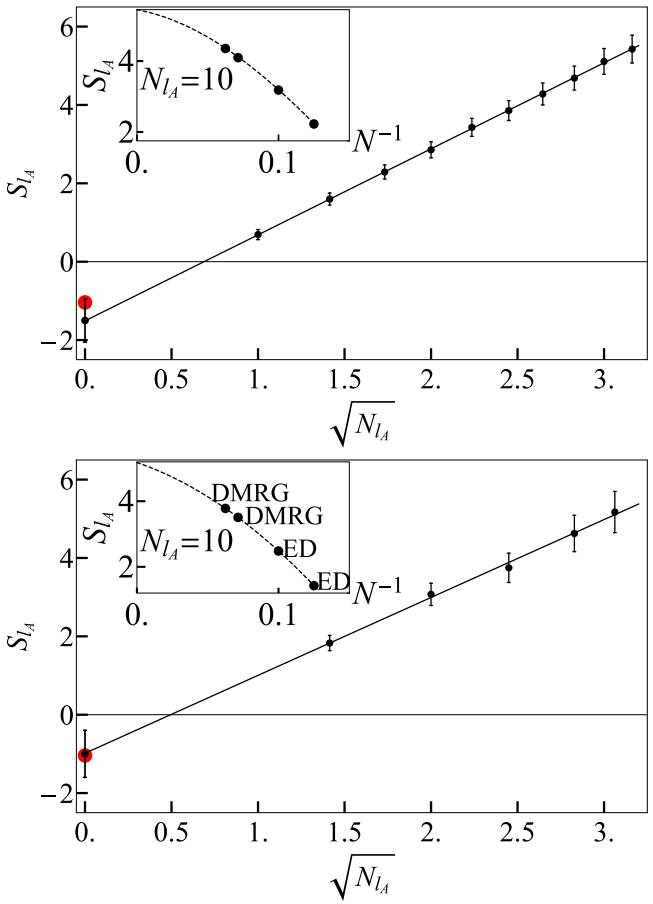

FIG. 4. Entanglement entropy for the single ground level basis (upper panel) and two-level basis (lower panel). The insets show fitting for $N_A = 10$ orbitals. Red dots: MR state.

We first compute the TEE for Hilbert space (i). Using the orbital partition, with block A including the first N_A orbitals near the south pole of the spherical shell, and other orbitals in block B, entanglement entropy is computed for $N = 8$, 10, 14, and 16 holes and $N_A = 2$–10 orbitals. For each number of orbitals, we obtain the thermodynamic limit of entanglement entropy by a parabolic fit of the data. This limit of S_A is linear in $\sqrt{N_A}$. The y intercept shows the topological part $-\Gamma$. A value of $\Gamma = 1.04$ corresponds to the MR state [50,52]. A numerical calculation for the MR state of electrons gives $\Gamma = 1.1 \pm 0.3$. Our result, $\Gamma_1 = 1.4 \pm 0.4$, agrees well with these values, indicating a MR state, as shown in the upper panel of Fig. 4.

For holes populating the two lowest levels [case (ii)], we use the density matrix renormalization group (DMRG) for $N = 14$ and 16, because very large Hilbert spaces make exact diagonalization difficult. We start with a few orbitals of the spherical shell, dividing the system into L and R parts. Adding orbitals between them, $L \bullet\bullet R$, we obtain the ground-state density matrix. Tracing it over $\bullet R$ and diagonalizing the reduced part, we retain up to 2000 states with the largest eigenvalues, forming the basis L used in the next iteration. The procedure stops when the required accuracy is reached [54,55]. Here, we obtain $\Gamma_2 = 1.0 \pm 0.4$, as shown in the lower panel of Fig. 4. This value is larger than $\ln\sqrt{6} \approx 0.9$, where 6 is the degeneracy of the MR state on the torus, indicating a non-Abelian state [50].

Conclusion. We proposed a method to study the quantum Hall hole systems in a spherical shell geometry. We demonstrate the incompressible FQH state at $\nu = \frac{1}{2}$ of the hole ground state in a magnetic field. The hole liquid at $\nu = \frac{1}{2}$ is not in the Halperin 331 state but is described by the Moore-Read-like correlations, with a sizable overlap of the wave functions of hole excitations and the Moore-Read Pfaffian excitations. The topological entanglement entropy indicates the non-Abelian character of the correlations for the $\nu = \frac{1}{2}$ hole state. Experimentally, besides direct interference tests aimed at the discovery of non-Abelian statistics [1,6], it is interesting to compare the transport characteristics and response to hydrostatic pressure [56] of the $\nu = \frac{1}{2}$ hole state and the $\nu = \frac{5}{2}$ electron state in high magnetic fields.

Acknowledgment. This work is supported by the U.S. Department of Energy, Office of Basic Energy Sciences, Division of Materials Sciences and Engineering under Award No. DE-SC0010544.

[1] C. Nayak, S. H. Simon, A. Stern, M. Freedman, and S. Das Sarma, Rev. Mod. Phys. **80**, 1083 (2008).
[2] L. Hormozi, N. E. Bonesteel, and S. H. Simon, Phys. Rev. Lett. **103**, 160501 (2009).
[3] S. Das Sarma, M. Freedman, and C. Nayak, Phys. Rev. Lett. **94**, 166802 (2005).
[4] G. Moore and N. Read, Nucl. Phys. B **360**, 362 (1991).
[5] N. Read and D. Green, Phys. Rev. B **61**, 10267 (2000).
[6] R. L. Willett, Rep. Prog. Phys. **76**, 076501 (2013).
[7] R. Willett, J. P. Eisenstein, H. L. Störmer, D. C. Tsui, A. C. Gossard, and J. H. English, Phys. Rev. Lett. **59**, 1776 (1987).
[8] W. Pan, J. S. Xia, H. L. Stormer, D. C. Tsui, C. Vicente, E. D. Adams, N. S. Sullivan, L. N. Pfeiffer, K. W. Baldwin, and K. W. West, Phys. Rev. B **77**, 075307 (2008).
[9] N. Samkharadze, J. D. Watson, G. Gardner, M. J. Manfra, L. N. Pfeiffer, K. W. West, and G. A. Csáthy, Phys. Rev. B **84**, 121305 (2011).
[10] N. Read and E. Rezayi, Phys. Rev. B **59**, 8084 (1999).
[11] E. Ardonne, F. J. M. van Lankvelt, A. W. W. Ludwig, and K. Schoutens, Phys. Rev. B **65**, 041305 (2002).
[12] M. Barkeshli and X.-G. Wen, Phys. Rev. Lett. **105**, 216804 (2010).
[13] D. R. Luhman, W. Pan, D. C. Tsui, L. N. Pfeiffer, K. W. Baldwin, and K. W. West, Phys. Rev. Lett. **101**, 266804 (2008).
[14] Z. Papić, G. Möller, M. V. Milovanović, N. Regnault, and M. O. Goerbig, Phys. Rev. B **79**, 245325 (2009).
[15] Y. W. Suen, L. W. Engel, M. B. Santos, M. Shayegan, and D. C. Tsui, Phys. Rev. Lett. **68**, 1379 (1992).
[16] S. Hasdemir, Y. Liu, H. Deng, M. Shayegan, L. N. Pfeiffer, K. W. West, K. W. Baldwin, and R. Winkler, Phys. Rev. B **91**, 045113 (2015).
[17] M. R. Peterson and S. Das Sarma, Phys. Rev. B **81**, 165304 (2010).

[18] Z. Papić, M. O. Goerbig, N. Regnault, and M. V. Milovanović, Phys. Rev. B **82**, 075302 (2010).
[19] D. P. Arovas and Y. Lyanda-Geller, Phys. Rev. B **57**, 12302 (1998).
[20] G. E. Simion and Y. B. Lyanda-Geller, Phys. Rev. B **90**, 195410 (2014).
[21] S.-R. E. Yang, A. H. MacDonald, and D. Yoshioka, Phys. Rev. B **41**, 1290 (1990).
[22] G. E. Simion and J. J. Quinn, Physica E **41**, 1 (2008).
[23] M. Levin, B. I. Halperin, and B. Rosenow, Phys. Rev. Lett. **99**, 236806 (2007).
[24] A. Wójs, C. Tőke, and J. K. Jain, Phys. Rev. Lett. **105**, 096802 (2010).
[25] G. J. Sreejith, C. Tőke, A. Wójs, and J. K. Jain, Phys. Rev. Lett. **107**, 086806 (2011).
[26] A. C. Archer and J. K. Jain, Phys. Rev. Lett. **110**, 246801 (2013).
[27] G. J. Sreejith, Y.-H. Wu, A. Wójs, and J. K. Jain, Phys. Rev. B **87**, 245125 (2013).
[28] A. C. Balram, C. Tőke, A. Wójs, and J. K. Jain, Phys. Rev. B **91**, 045109 (2015).
[29] F. D. M. Haldane, Phys. Rev. Lett. **51**, 605 (1983).
[30] B. I. Halperin, Helv. Phys. Acta **56**, 75 (1983).
[31] J. M. Luttinger, Phys. Rev. **102**, 1030 (1956).
[32] L. Landau and E. Lifshitz, *Quantum Mechanics* (Butterworth-Heinemann, Oxford, UK, 1981).
[33] A. Wójs and J. J. Quinn, Phys. Rev. B **75**, 085318 (2007).
[34] T. T. Wu and C. N. Yang, Nucl. Phys. B **107**, 365 (1976).
[35] A. Edmonds, *Angular Momentum in Quantum Mechanics* (Princeton University Press, Princeton, NJ, 1996).
[36] S. H. Simon and E. H. Rezayi, Phys. Rev. B **87**, 155426 (2013).
[37] R. E. Wooten, J. H. Macek, and J. J. Quinn, Phys. Rev. B **88**, 155421 (2013).
[38] The cyclotron frequency ω_C corresponds to the semiclassical cyclotron frequency at large n [20].
[39] E. H. Rezayi and F. D. M. Haldane, Phys. Rev. B **42**, 4532 (1990).
[40] See Supplemental Material at http://link.aps.org/supplemental/10.1103/PhysRevB.95.161111 for pseudopotentials, interaction matrix elements, and equations for $R^l_{\alpha j}(r)$.
[41] X. G. Wen and A. Zee, Phys. Rev. Lett. **69**, 953 (1992).
[42] N. d'Ambrumenil and R. Morf, Phys. Rev. B **40**, 6108 (1989).
[43] M. Storni, R. H. Morf, and S. Das Sarma, Phys. Rev. Lett. **104**, 076803 (2010).
[44] Y. Liu, A. L. Graninger, S. Hasdemir, M. Shayegan, L. N. Pfeiffer, K. W. West, K. W. Baldwin, and R. Winkler, Phys. Rev. Lett. **112**, 046804 (2014).
[45] F. D. M. Haldane and E. H. Rezayi, Phys. Rev. Lett. **60**, 956 (1988).
[46] T. Ho, Phys. Rev. Lett. **75**, 1186 (1995).
[47] M. Greiter, X.-G. Wen, and F. Wilczek, Phys. Rev. Lett. **66**, 3205 (1991).
[48] M. Haque, O. S. Zozulya, and K. Schoutens, Phys. Rev. Lett. **98**, 060401 (2007).
[49] P. Fendley, M. P. A. Fisher, and C. Nayak, J. Stat. Phys. **126**, 1111 (2007).
[50] O. S. Zozulya, M. Haque, K. Schoutens, and E. H. Rezayi, Phys. Rev. B **76**, 125310 (2007).
[51] Z.-X. Hu, Z. Papi, S. Johri, R. N. Bhatt, and P. Schmitteckert, Phys. Lett. A **376**, 2157 (2012).
[52] A. Kitaev and J. Preskill, Phys. Rev. Lett. **96**, 110404 (2006).
[53] M. P. Zaletel, R. S. K. Mong, and F. Pollmann, Phys. Rev. Lett. **110**, 236801 (2013).
[54] A. E. Feiguin, E. Rezayi, C. Nayak, and S. Das Sarma, Phys. Rev. Lett. **100**, 166803 (2008).
[55] M. P. Zaletel, R. S. K. Mong, F. Pollmann, and E. H. Rezayi, Phys. Rev. B **91**, 045115 (2015).
[56] N. Samkharadze, K. Schreiber, G. Gardner, M. J. Manfra, E. Fradkin, and G. A. Csáthy, Nat. Phys. **12**, 191 (2016).